[4] M. Li, Y. Yin, W.-B. Zhang, K. Zhou, and H. Nakamura, "Modeling and implementation of adaptive transit signal priority on actuated control systems," *Comput.-Aided Civil Infrastruct. Eng.*, vol. 26, no. 4, pp. 270–284, May 2011.
[5] K. Wang and Z. Shen, "Artificial societies and GPU-based cloud computing for intelligent transportation management," *IEEE Intell. Syst.*, vol. 26, no. 4, pp. 22–28, Jul./Aug. 2011.
[6] K. F. Petty, P. Bickel, M. Ostland, J. Rice, F. Schoenberg, J. Jiang, and Y. A. Ritov, "Accurate estimation of travel times from single-loop detectors," *Transp. Res. A, Policy Pract.*, vol. 32, no. 1, pp. 1–17, Jan. 1998.
[7] A. Polus, "A study of travel time and reliability on arterial routes," *Transportation*, vol. 8, no. 2, pp. 141–151, Jun. 1979.
[8] J. W. H. Van Lint, "Empirical evaluation of new robust travel time estimation algorithms," *Transp. Res. Rec.*, vol. 2160, pp. 50–59, 2010.
[9] C. D. R. Lindveld, R. Thijs, P. H. L. Bovy, and N. J. Van der Zijpp, "Evaluation of online travel time estimators and predictors," *Transp. Res. Rec.*, no. 1719, pp. 45–53, Feb. 2000.
[10] B. L. Vanajakshi, "Estimation and prediction of travel time from loop detector data for intelligent transportation systems applications," Ph.D. dissertation, Dept. Civil Eng., Texas A&M Univ., College Station, TX, USA, 2004.
[11] R. Li, G. Rose, and M. Sarvi, "Evaluation of speed-based travel time estimation models," *ASCE J. Transp. Eng.*, vol. 132, no. 7, pp. 540–547, Jul. 2006.
[12] Q. Ou, J. W. C. van Lint, and S. P. Hoogendoorn, "Piecewise inverse speed correction by using individual travel times," *Transp. Res. Rec.*, vol. 2049, pp. 92–102, Feb. 2008.
[13] F. Soriguera, "Requiem for freeway travel time estimation methods based on blind speed interpolations between point measurements," *IEEE Trans. Intell. Transp. Syst.*, vol. 12, no. 1, pp. 291–297, Mar. 2011.
[14] H. M. Zhang and W. Shen, "Numerical investigation of stop-and-go traffic patterns upstream of freeway lane drop," *Transp. Res. Rec.*, vol. 2124, pp. 3–17, Feb. 2009.
[15] Next Generation SIMulation (NGSIM). [Online]. Available: http://ngsim-community.org/
[16] D. H. Nam and D. R. Drew, "Automatic measurement of traffic variable for intelligent transportation systems applications," *Transp. Res. B, Methodol.*, vol. 33, no. 6, pp. 437–457, Aug. 1999.
[17] J. W. C. van Lint, "Reliable travel time prediction for freeways," Ph.D. dissertation, Delft Univ. Technol., Delft, The Netherlands, 2004.
[18] D. Ni and H. Wang, "Trajectory reconstruction for travel time estimation," *J. Intell. Transp. Syst.*, vol. 12, no. 3, pp. 113–125, Aug. 2008.
[19] P. Izadpanah, B. Hellinga, and L. Fu, "Real-time freeway travel time prediction using vehicle trajectory data," in *Proc. 90th Annu. Meeting Transp. Res. Board*, Washington, DC, USA, 2011.
[20] Z. Chen, C. Yang, and A. Chen, "Estimating fuel consumption and emissions based on reconstructed vehicle trajectories," *J. Adv. Transp.*, in press.
[21] B. Coifman, "Estimating travel times and vehicle trajectories on freeways using dual loop detectors," *Transp. Res. A, Policy Pract.*, vol. 36, no. 4, pp. 351–364, May 2002.
[22] B. Coifman and M. Cassidy, "Vehicle reidentification and travel time measurement on congested freeways," *Transp. Res. A, Policy Pract.*, vol. 36, no. 10, pp. 899–917, Dec. 2002.
[23] B. Mehran, M. Kuwahara, and F. Naznin, "Implementing kinematic wave theory to reconstruct vehicle trajectories from fixed and probe sensor data," *Transp. Res. C, Emerg. Technol.*, vol. 20, no. 1, pp. 144–163, Feb. 2012.
[24] X. Chen, Z. Li, and L. Li, "Phase diagram analysis based on a temporal–spatial queueing model," *IEEE Trans. Intell. Transp. Syst.*, vol. 13, no. 4, pp. 1705–1716, Dec. 2012.
[25] X. Chen, L. Li, and Y. Zhang, "A Markov model for headway/spacing distribution of road traffic," *IEEE Trans. Intell. Transp. Syst.*, vol. 11, no. 4, pp. 773–785, Dec. 2010.
[26] L. Li, X. Chen, and Z. Li, "Asymmetric stochastic Tau theory in car-following," *Transp. Res. F, Traffic Psychol. Behav.*, vol. 18, pp. 21–23, May 2013.
[27] A. A. Kurzhanskiy and P. Varaiya, "Guaranteed prediction and estimation of the state of a road network," *Transp. Res. C, Emerg. Technol.*, vol. 21, no. 1, pp. 163–180, Apr. 2012.
[28] G. McLachlan and T. Krishnan, *The EM Algorithm and Extensions,* 2nd ed. Hoboken, NJ, USA: Wiley, 2008.

UTN-Model-Based Traffic Flow Prediction for Parallel-Transportation Management Systems

Qing-Jie Kong, *Member, IEEE*, Yanyan Xu, Shu Lin, *Member, IEEE*, Ding Wen, *Senior Member, IEEE*, Fenghua Zhu, *Member, IEEE*, and Yuncai Liu, *Member, IEEE*

***Abstract*—Aiming to comply with the requirement of parallel-transportation management systems (PtMS), this paper presents a short-term traffic flow prediction method for signal-controlled urban traffic networks (UTNs) based on the macroscopic UTN model. In contrast with other time-series-based or spatio-temporal correlation methods, the proposed method focuses more on using the substantial mechanism of traffic transmission in road networks and the topology model of the entire UTN. Furthermore, this approach employs a speed-density model based on the fundamental diagram (FD) to obtain more accurate travel times in links. In the comparison experiment, the microscopic traffic simulation software CORSIM is adopted to simulate the real urban traffic. The experiment results fully verify the outstanding performances of the proposed prediction method.**

***Index Terms*—CORSIM, fundamental diagram (FD), parallel-transportation management systems (PtMS), short-term traffic flow prediction, urban traffic network (UTN) model.**

I. Introduction

Parallel-transportation management systems (PtMS) have been recently proposed and verified in the real world, as a novel and effective solution for modeling, analysis, and control of complex urban traffic systems [1], [2]. PtMS consist of five major components: 1) actual transportation systems; 2) artificial transportation systems (ATS); 3) traffic operator and administrator training systems (OTS*t*); 4) decision evaluation and validation systems (Dyna*CAS*); and 5) traffic sensing, control, and management systems (*a*DAPTS).

However, when we develop and apply PtMS in engineering practice, some related intelligent transportation systems theory and technologies face new challenges. For instance, in the fourth component of PtMS, i.e., Dyna*CAS*, emerging traffic patterns need to be accurately predicted based on computational modeling of traffic flow, road, and environments involved in transportation activities. However, the existing traffic prediction models are seldom built based on the mechanism of traffic moving in road networks and the impact of the related environment factors, but they always focus on fitting the change

Manuscript received July 6, 2012; revised December 15, 2012; accepted March 8, 2013. Date of publication March 28, 2013; date of current version August 28, 2013. This work was supported in part by the National Natural Science Foundation of China Program under Grant 61104160, Grant 61203169, Grant 61174172, Grant 61233001, and Grant 71232006, by the National 863 Key Program of China under Grant 2012AA112307, and by Science and Technology Commission of Shanghai Municipality Program under Grant 11231202801. The Associate Editor for this paper was L. Li.

Q.-J. Kong and F. Zhu are with the State Key Laboratory for Management and Control of Complex Systems, Institute of Automation, Chinese Academy of Sciences, Beijing 100190, China (e-mail: kongqingjie@gmail.com; fenghua.zhu@ia.ac.cn).

Y. Xu, S. Lin, and Y. Liu are with the Department of Automation, Shanghai Jiao Tong University, Shanghai 200240, China (e-mail: xustone@sjtu.edu.cn; lisashulin@gmail.com; whomliu@sjtu.edu.cn).

D. Wen is with the Center for Military Computational Experiments and Parallel Systems Technology, National University of Defense Technology, Changsha, 410073, China (e-mail: wending2010@gmail.com).

Color versions of one or more of the figures in this paper are available online at http://ieeexplore.ieee.org.

Digital Object Identifier 10.1109/TITS.2013.2252463

1524-9050 © 2013 IEEE

tendency of traffic flow with some function tools based on historical data or upstream links. This situation can be reflected by the following review.

Short-term traffic flow prediction has been deeply studied for several decades, as one of the key technologies for advanced traffic management and traveler information services. Since the early 1980s, researchers have employed the historical data to predict short-term traffic flow by different methods, mostly in freeways, e.g., prediction through Kalman filtering [3], the nonparametric regression method [4], the autoregressive integrated moving average (ARIMA) [5], the artificial-neural-network approach [6], the fuzzy logic-based method [7], etc. By considering the traffic flow as time series, these approaches can mostly perform well on a freeway or a location on an urban artery, instead of the whole complicated urban-road network. In the recent years, approaches that are incorporating temporal and spatial characteristics have been presented to predict urban traffic flow. Sun *et al.* [8] proposed the approach based on the Bayesian network, which takes account of historical data from both current and neighbor junctions to achieve better effectiveness. Vlahogianni *et al.* [9] proposed multilayer perceptions that were fed with volume data from sequential locations to improve the accuracy of short-term forecasts. Min and Wynter [10] predicted road traffic by taking into account the spatial characteristics of a road network, which contain not only the distances but the average speeds in the links as well.

Because of the consideration of the operation mechanism of the network traffic flow, these aforementioned methods can usually obtain good effect only in normal traffic statuses, i.e., the traffic flow smoothly or gradually changes, whereas they often generate inaccurate predictions when the traffic flow suddenly changes. In this case, these existing prediction methods cannot yet satisfy the requirement of urban PtMS in accuracy. To better realize PtMS in the urban-road network, in this paper, we propose a novel approach, which is based on the macroscopic urban traffic network (UTN) model [11], [12], to implement the short-term traffic flow prediction. This UTN-model-based approach has two distinguished advantages over the traditional methods.

1) The UTN model is built according to the transmission pattern of the traffic flow in the object road network and can thereby veritably reflect the operation mechanism of the traffic flow.
2) The prediction model can easily integrate the environment factors that are impacting the traffic flow, such as traffic signal, turning rate, and input/output flow to obtain better prediction performances.

Therefore, using the UTN-model-based prediction method, Dyna*CAS* can obtain better results of traffic flow prediction, which can greatly improve the performance of urban PtMS.

This paper is structured as follows: Section II specifies the UTN, the urban topology, and the signalized link model. In addition, the speed-density model method is also presented to obtain the link average speed in the UTN model. A simulation case study is expounded in Section III. Some concluding remarks and directions for the future work are given in Section IV.

II. Urban Traffic Network Model

In this section, the UTN [12] and link models [13] are briefly introduced; furthermore, some improvements are employed to make the UTN model more accurate.

Considering the models that are described in the following sections, the notations are listed in Table I.

TABLE I
NOTATIONS DEFINED IN THE UTN MODEL

Symbol	Description
T	sampling time interval (sec)
$D \in \{W, N, E, S\}$	orientation of the link in the network element (i.e. *west, north, east, south*)
$t \in \{s, l, r\}$	direction of the traffic turn movement in the link (i.e. *straight, left, right*)
$v_D^0(i,j)$	free flow speed in the link (m/s)
$v_D(i,j,k)^*$	average flow speed in the link from link entrance to tail of the queue (km/h)
$C_D(i,j)$	capacity of the link (veh)
$W_D(i,j)$	number of lanes in the link
L_{veh}	average length of vehicles (m)
$t_h{}^*$	mean discharge headway (sec)
s_{Dt}	saturated flow rate turning t (veh/s)
$\beta_{Dt}(i,j,k)$	turning rate at the stop line in the link at time k
$d_{Dt}(i,j,k)$	number of vehicles discharge from the link to t at time k (veh)
$d_{in,D}(i,j,k)$	number of vehicles enter the link at time k (veh)
$d_{out,D}(i,j,k)$	number of vehicles depart from the link at time k (veh)
$x_D(i,j,k)$	number of vehicles waiting in the link at time k (veh)
$a_D(i,j,k)$	number of vehicles arriving at the tail of the waiting queue in the link at time k (veh)
$f_D(i,j,k)$	available free space in the link at time k (veh)
$f_{Dt,dsl}(i,j,k)$	free space in the downstream link of the departure vehicles turning t at the time k (veh)
$r_D(i,j,k)^*$	density of vehicles in the link at time t (veh/m)
$r_{jam,D}(i,j)^*$	jam density in the link (veh/m)
$q_D(i,j,k)^*$	flow rate in the link at time t (veh/s)
$q_{m,D}(i,j)^*$	maximum flow rate in the link (veh/s)
$g_{Dt}(i,j,k)$	signal symbol for vehicles turning t, 1 when signal is green, 0 when signal is red

* : Extra parameters in the improved UTN model.

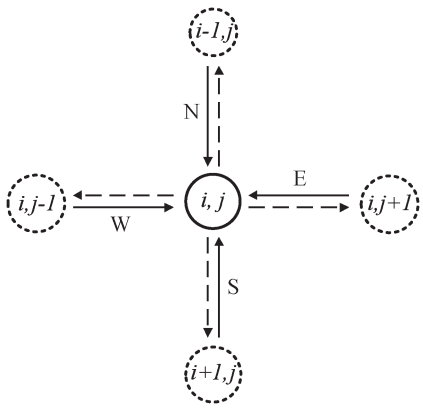

Fig. 1. Urban traffic network element.

A. Node Model

According to the topology of the UTN, it is decomposed into three types of network elements, i.e., junction nodes, source nodes, and all links pointing to it, as shown in Fig. 1. Then, the whole UTN can be constructed by assembling these elements together. The basic UTN that is shown in Fig. 2 is a network with five lines and five columns and is made up of three sorts of network elements, i.e., "Cross," "T-shape," and "Source." "Cross" is a normal element with four coming links,

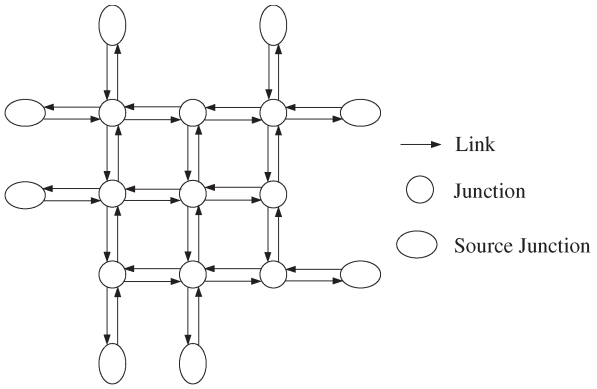

Fig. 2. Basic UTN.

"T-shape" elements contain three coming links, and "Source" elements are the elements where traffic flows get in and out of the network. Among them, "T-shape" and "Source" are further categorized by their directions.

Cross is the typical calculating element in the UTN model, which contains a node and joint links running to it as the solid lines shown in Fig. 1. The signalized junction of the UTN element is defined by the coordinates in the form of (i, j) (i and j represent the line and column numbers of the node). The links assembling to the junction are labeled by their orientations, i.e., west (W), south (S), east (E), and north (N) links. The whole UTN element is marked as $E(i, j)$. Once the types and the coordinates of the network elements are given, the topology of an urban-road network can be fixed.

After building the UTN element model, the macroscopic traffic behavior at the signalized junction can be represented by mathematical formula. Thus, for any link D of $E(i, j)$, the number of the departure vehicles turning t is given by (1), shown at the bottom of the page, where $x_{Dt}(i, j, k)$ is the number of the vehicles that are waiting in link D and turning t at time k, and $a_{Dt}(i, j, k)$ is the number of the vehicles that are arriving at end of the tail of the link.

Both of them are expressed by the predefined turning rate as follows:

$$\begin{cases} x_{Dt}(i,j,k) = x_D(i,j,k)\beta_{Dt}(i,j,k) \\ a_{Dt}(i,j,k) = a_D(i,j,k)\beta_{Dt}(i,j,k). \end{cases} \tag{2}$$

In (1), $s_{Dt}(i, j)$, which is the maximal number of vehicles that can pass the junction turning t in the link, is calculated by the mean discharge headway t_h when the vehicle leaves the stop line at the end of the link [see (3), shown below]. To obtain a good approximation to the real traffic, it is differentiated that the vehicles that turn left or right will queue in the leftmost or rightmost lane, whereas the vehicles that go straight can wait in the lanes left, i.e.,

$$s_{Dt}(i,j) = \begin{cases} 1/t_h, & \text{if } t = \{l, r\} \\ 1/t_h \cdot (W_D(i,j) - 1), & \text{if } t = s, \text{T-shape} \\ 1/t_h \cdot (W_D(i,j) - 2), & \text{if } t = s, \text{Cross.} \end{cases} \tag{3}$$

B. Link Model

The link model that we used is based on the model proposed by Berg *et al.* [13]. To simulate the real road link, a basic diagram of the road segment between two signalized junctions is represented as Fig. 3.

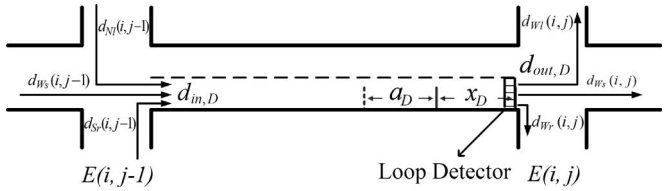

Fig. 3. UTN link model.

In the process of vehicle transmission in a link, we assume that there is no vehicle access or that it disappears in the road segment. In another words, all vehicles that enter a link will depart the link after a period of time. Based on this assumption, the free space in link D of $E(i, j)$ is updated by

$$f_D(i,j,k+1) = f_D(i,j,k) - d_{\text{in},D}(i,j,k) + d_{\text{out},D}(i,j,k) \tag{4}$$

where

$$\begin{cases} d_{\text{out},D}(i,j,k) = d_{Ds}(i,j,k) + d_{Dl}(i,j,k) + d_{Dr}(i,j,k) \\ d_{\text{in},D}(i,j,k) = \sum_{D_u \in D_{\text{upl}}} d_{D_u,D}(i,j,k) \end{cases} \tag{5}$$

in which D_{upl} represents the set of upstream links of link D, and $d_{D_u,D}(i, j, k)$ means the number of vehicles that depart from upstream link D_u to link D at time k.

We can represent the number of vehicles arriving at the tail of the waiting queues in link D of $E(i, j)$ as follows:

$$\begin{aligned} a_D(i,j,k) = &\left(\frac{T - \gamma_D(i,j,k)}{T}\right) d_{\text{in},D}\left(i,j,k - \delta_D(i,j,k) - \sigma\right) \\ &+ \left(\frac{\gamma_D(i,j,k)}{T}\right) d_{\text{in},D}\left(i,j,k - \delta_D(i,j,k) - 1 - \sigma\right) \end{aligned} \tag{6}$$

where

$$\begin{cases} \delta_D(i,j,k) = \text{fix}\left(\frac{(C_D(i,j) - x_D(i,j,k))L_{\text{veh}}}{W_D(i,j)v_D(i,j,k)T}\right) \\ \gamma_D(i,j,k) = \text{rem}\left(\frac{(C_D(i,j) - x_D(i,j,k))L_{\text{veh}}}{W_D(i,j)v_D(i,j,k)T}\right) \end{cases} \tag{7}$$

and σ represents the time during which the vehicles freely pass through the junction. In (7), $\text{fix}(x/y)$ represents the quotient of equation x/y, and $\text{rem}(x/y)$ represents the remainder.

Finally, the number of vehicles that are waiting in the queue turning t in link D of $E(i, j)$ is updated by

$$\begin{aligned} x_{Dt}(i,j,k+1) = &\, x_{Dt}(i,j,k) + \beta_{Dt}(i,j,k) \\ &\times a_D(i,j,k) - d_{Dt}(i,j,k). \end{aligned} \tag{8}$$

In the previous model proposed in [12], the delay time of the vehicles that are running from the beginning of link D to the tail of the queues was calculated by (7). Then, the average speed of the vehicles in link D from the beginning to the tail of the queue was regarded as the free-flow speed. However, vehicles cannot always keep free-flow speed $v_D^0(i, j)$ on the link, which is particularly located in a high-density segment. To obtain a more precise prediction, we amend the

$$d_{Dt}(i,j,k) = \begin{cases} \min\left\{x_{Dt}(i,j,k) + a_{Dt}\left(i,j,k\right)\right), f_{Dt,dsl}(i,j,k), s_{Dt}(i,j)T\right\}, & \text{if } g_{Dt}(i,j,k) = 1 \\ 0, & \text{if } g_{Dt}(i,j,k) = 0 \end{cases} \tag{1}$$

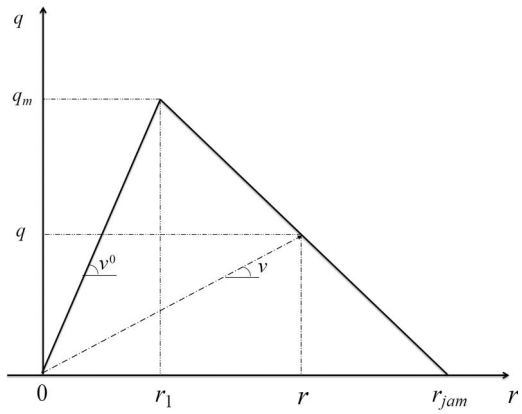

Fig. 4. Triangular-shaped FD.

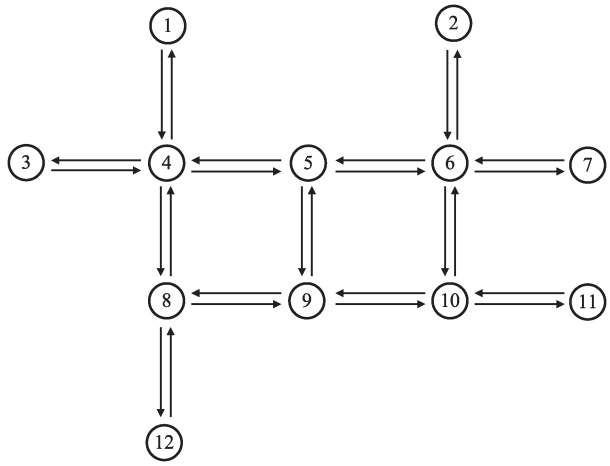

Fig. 5. Urban traffic network simulated in the experiment.

average speed $v_D(i,j,k)$ based on the speed-density model, which is described in the next subsection.

C. Speed-Density Model

In this section, we apply a speed-density model based on the fundamental diagram (FD) [16], [17] into the link model to make the estimated travel time closer to the real traffic situation. From the speed-density FD, we can derive a function for the travel speed of the traffic flows on a road with respect to the traffic density on the road. With the derived travel speed, we can make a more accurate estimate of the travel time for traffic flows that are moving inside the link before reaching the waiting queues.

Classical forms of the FD are the triangular and parabolic shapes. For the sake of simple and effective calculation, we adopt the triangular-shaped FD, as shown in Fig. 4. In our case, the FD is defined by three values: the maximum flow rate (maximum number of vehicles through the link per hour) q_m, the traffic jam density $r_{\rm jam}$ of the link, and velocity v^0 in the free-flow state.

The triangular-shaped curve shown in Fig. 4 consists of two vectors. One is the free-flow side of the curve, in which the velocity is equal to the free-flow speed v^0. The other vector is the congested branch, which starts with the maximum flow rate q_m to the state with zero flow and jam density $r_{\rm jam}$. The congested branch has a negative slope, which implies that the higher the density on the congested branch, the lower the flow rate, and it dovetails with the real traffic condition. The vertex of the triangular-shaped FD (r_1, q_m) can be obtained by

$$r_1 = q_m(i,j)/v_D^0(i,j). \tag{9}$$

Based on this diagram, relationships between vehicle density, flow rate, and average velocity can be described by

$$q(i,j) = \begin{cases} v_D^0(i,j)r & 0 \le r < r_1 \\ -\frac{q_m}{r_{\rm jam}-r_1}r + \frac{q_m r_{\rm jam}}{r_{\rm jam}-r_1} & r_1 \le r \le r_{\rm jam} \end{cases} \tag{10}$$

where $r = [1 - f_D(i,j,k)/C_D(i,j)]/L_{\rm veh}$, $r_{\rm jam} = W_D(i,j)/L_{\rm veh}$, and $q_m = W_D(i,j)/t_h$. Then, the average speed in link D of $E(i,j)$ at time k can be calculated as follows:

$$v_D(i,j,k) = \frac{q}{r} = \begin{cases} v_D^0(i,j) & 0 \le r < r_1 \\ \frac{q_m v_D^0(i,j)}{r_{\rm jam} v_D^0(i,j) q_m} \cdot \frac{r_{\rm jam}-r}{r} & r_1 \le r \le r_{\rm jam}. \end{cases} \tag{11}$$

The average speed is equal to the free-flow speed, when the traffic density belongs to the free-flow region (left branch) of the FD; the value of the average speed depends on the average density, when the traffic density is in the congested region (right branch) of the FD.

Finally, we update $v_D(i,j,k)$ in (7) to implement more accurate estimation to the vehicle delay time in the link.

III. Experiment Design and Result Discussion

In this paper, to evaluate the prediction approach based on the macroscopic road network model, the traffic simulation software package TSIS-CORSIM, which was exploited by the Federal Highway Administration [14], is employed to simulate the real-world urban surface road traffic. The simulation results are treated as the ground truth. Consequently, the UTN model can be taken as the parallel model of the simulation traffic network to provide the traffic prediction results.

Same as many dynamic urban traffic models, the UTN model requires a lot of information. The information can be classified into three categories: 1) the information that can be directly obtained from the traffic network infrastructures (e.g., network topology and signal settings); 2) the information that needs to be further estimated/predicted (e.g., future network input demands and turning rates); and 3) the information that needs to be calibrated and can be applied as fixed parameters/features (e.g., discharge headway, link capacity, mean vehicle length, and FD parameters). Information type 1 will not introduce errors. In the simulations, we could input the same future network input demands and turning rates for CORSIM and the UTN model. Thus, the noises and the errors caused by information type 2 can be eliminated from the simulations. For information type 3, the discharge headway is obtained from CORSIM data; the link capacity, the mean vehicle length, and the FD parameters are calibrated by the CORSIM simulation, where an urban road is made to be fully congested.

A. Experiment Design

For the purpose of simulating the traffic flow in an urban surface road network, an example of UTNs is built and executed in CORSIM, as shown in Fig. 5. The experiment continues for 18 h under some predetermined parameters. The proposed prediction model reads the traffic states in all of the road links every 5 min and then predicts the traffic flow in the future 5 min using the detected traffic states and the property of the road network.

The details of the experiment design are expatiated as follows. First, the signal information (i.e., cycle length, offset time, phase, split, etc.) at each intersection are fixed and predefined. Then, the statistical average of the traffic flows that are feeding into the road network at the

TABLE II
PREDICTION ERRORS FOR THE THREE TYPICAL LINKS

	Link $(1,4)$	Link $(5,9)$	Link $(8,9)$
MAPE	0.045225	0.16013	0.13402
MASE	0.50752	0.87701	0.74548

source junctions (node 1, 2, 3, 7, 11, and 12) are predetermined as well. Furthermore, to represent the real complex traffic conditions and verify the effectiveness and the robustness of the proposed prediction model, the input traffic flows not only vary in a wide range but contain many noises as well. What deserves special mention is that the traffic flows feeding into the network follow a statistical average value instead of the precise input variables. Aside from that, the average vehicle length, the mean discharge headway, the time the vehicles pass through the junction, and the average turning percentages at the stop lines are all set to fixed values in the experiment.

When operating with the predefined parameters, the UTN model reads the current traffic states of the whole network from CORSIM every 5 min. Meanwhile, the UTN model lives completely outside the CORSIM simulation and operates in parallel. Moreover, the UTN model updates the traffic states of the road network every 1 s. Thus, after each 300-time updating, the UTN model calculates the average traffic flow in the 5 min, which denotes the mean traffic flow rate that is discharged from a link.

Finally, in the sample urban network that we studied, three typical links are selected to investigate the performances of the proposed prediction model, i.e., links (1,4), (5,9), and (8,9) in Fig. 5.

B. Results and Discussion

In the accuracy experiment, two criteria are employed to evaluate the prediction error of the proposed model. One is the mean absolute percentage error (MAPE); the other criterion is the mean absolute scaled error (MASE). Especially, the MASE is the measure of the forecast accuracy proposed by Hyndman and Koehler [15]. In contrast with the traditional error measures (e.g., the root-mean-square error and the MAPE), the MASE takes into account the gradient error between the prediction values and the actual values. Therefore, using the MASE, the prediction accuracy can be compared not only between different methods for the same link but between methods for different road links as well. Similarly, a smaller MASE indicates better prediction. The MAPE and the MASE are defined as follows:

$$\text{MAPE} = \frac{1}{K}\sum_{k=1}^{K}\frac{|V_k - \hat{V}_k|}{V_k} \tag{12}$$

$$\text{MASE} = \frac{1}{K}\sum_{k=1}^{K}\left|\frac{V_k - \hat{V}_k}{\frac{1}{K-1}\sum_{k=2}^{K}|V_k - V_{k-1}|}\right| \tag{13}$$

where K is the total number of intervals during the experiment, V_k denotes the average traffic flow generated by CORSIM and is treated as the actual value, and $\hat{V}_k$ is the prediction value that is produced by the proposed UTN model.

Table II shows the experimental results of three typical road links that are located in the border and the center of the road network. The prediction errors of all the road links are also shown in Fig. 6. Furthermore, Figs. 7–9 show the trend lines of the actual traffic flows that are produced by CORSIM and the predictive values that are produced by the proposed model.

In Fig. 6, it is shown that most of the links acceptably perform with the MAPE less than 0.15 and the average MAPE is equal to 0.133. From the perspective of the MASE, the average MASE of the links

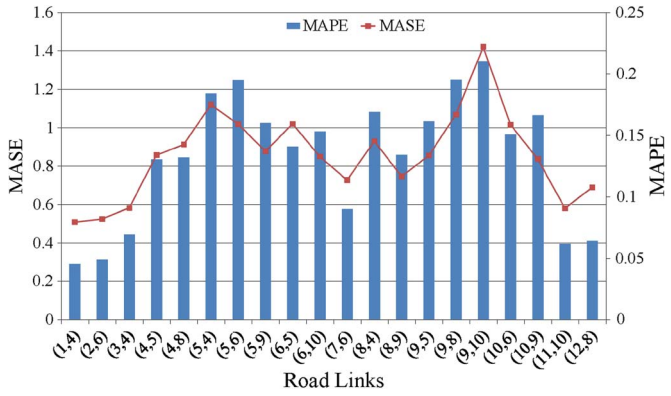

Fig. 6. Prediction errors for every link of the traffic network.

is 0.856, which indicates that the predictive results are acceptable, according to the criterion mentioned in [15]. Moreover, it is obviously observed that the prediction result in link (1,4) is much better than that in the other two links. As shown in Fig. 7, the traffic flows generated by the proposed prediction model maintain a high degree of unity with that of CORSIM. This result can really verify the effectiveness of the link transmission model, as the traffic flow in this link directly comes from the source junction and is not impacted by other factors, such as turning rates and waiting vehicles. Therefore, the average MAPE in the six links that are directly connected to the source junctions is as low as 0.063.

However, for the road links that are located in the center of the traffic network, the prediction accuracy of the UTN model is inferior to that for the marginal links (see Table II). Through intensive study on the proposed UTN model, we realize that such higher errors are caused by the predefined parameters of the model, i.e., the turning rates, the number of waiting vehicles, etc. On the contrary, the real-world urban surface traffic networks include many uncertainties, as does CORSIM. Furthermore, such impacts can constantly accumulate with the increasing number of passed links. In spite of this, the prediction curves of the UTN model are still able to follow the variation tendencies of the actual values, particularly at the time when the traffic states suddenly and greatly change. This advantage can be clearly observed not only in Fig. 7, which shows the result in the link near the source junction, but in Figs. 8 and 9 as well, which show the results in the center links. We can take Fig. 8 as an example to show this advantage. In Fig. 8, there are a sudden and huge increase in the traffic flow outputted by CORSIM from the 25th to 27th periods and a sudden and huge decrease from the 51th to 55th periods. For these sudden changes, the proposed prediction method gives accurate and rapid response. This performance is very valuable, as obtaining this performance is not very easy for most of the traditional methods. Moreover, it is worthy to mention that this prediction model considers no information about the historical data when performing prediction.

In the experiment, the UTN model was operated in a personal computer with a 2.8-GHz processor and 4-GB memory. The computing time for each prediction step is observed to vary between 1 and 2 central-processing-unit seconds for the whole network (shown in Fig. 5) in a small sampling time interval $T = 1\ s$. Obviously, larger sampling intervals can further reduce the computing cost. Therefore, the proposed prediction model can satisfy the requirement of real-time prediction.

Additionally, the flexibility and the robustness of prediction methods are both indispensable indicators aside from the accuracy and the operation speed in short-term traffic flow prediction. By combining the current observed traffic states and the inherent properties of road networks to predict the traffic flow in short term, the proposed prediction

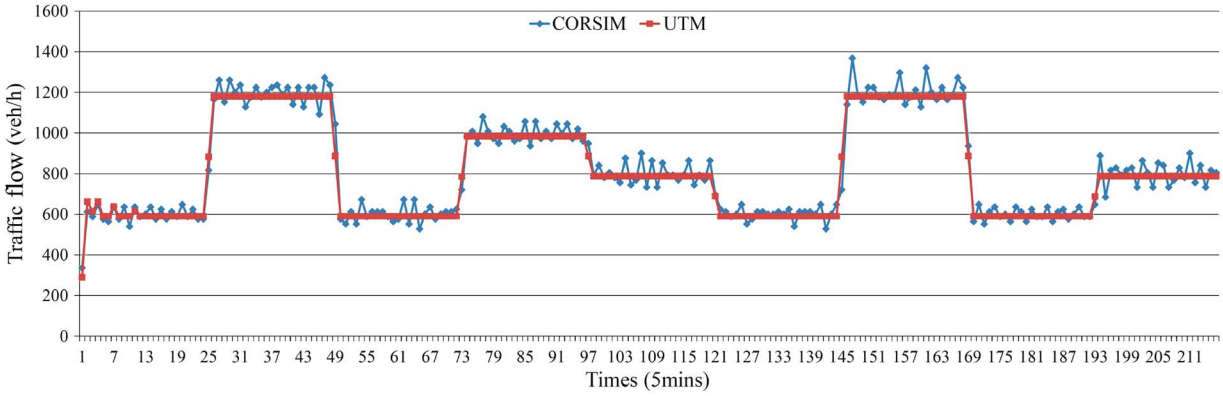

Fig. 7. Prediction of average traffic flow for link (1,4).

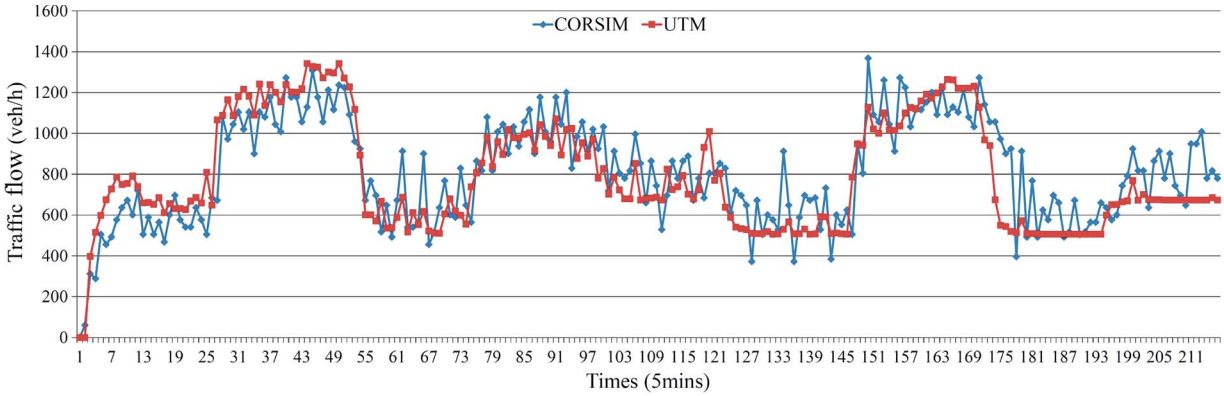

Fig. 8. Prediction of average traffic flow for link (5,9).

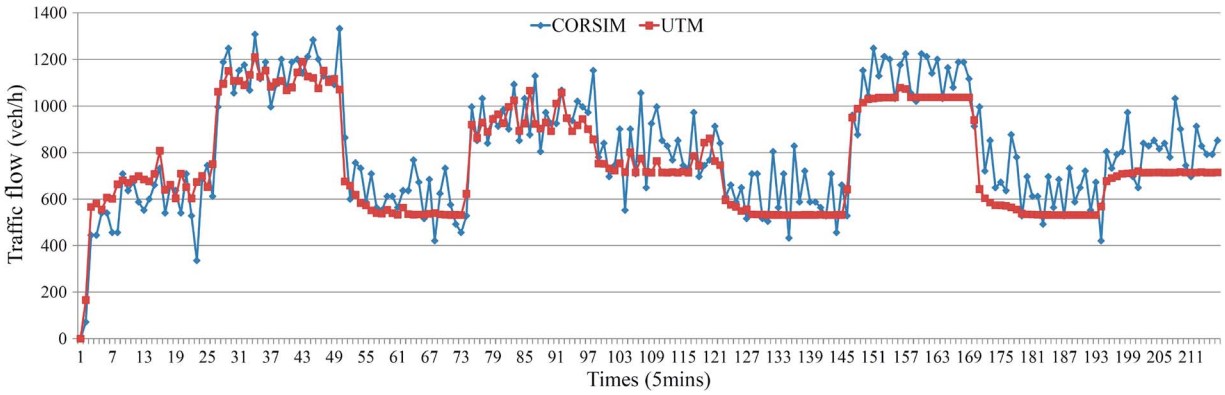

Fig. 9. Prediction of average traffic flow for link (8,9).

model can stably perform on weekdays and holidays and even while encountering special cases (e.g., severe weather, traffic accidents, or large assemblies).

IV. Conclusion and Future Work

This paper has presented a short-term traffic flow prediction approach based on the macroscopic UTN model for urban surface road network with signalized junctions. The proposed method is totally on the basis of the spatial structure of the UTN and the transmission mechanism of traffic flow. Furthermore, we have employed a simple speed-density model based on the triangular-shaped FD to obtain the more accurate approximation of the vehicle delay time from the beginning of links to the tail of queues. Finally, the comparison experiments with CORSIM indicate that the proposed model can timely and accurately predict the short-term traffic flow, even during sudden state changes and traffic peaks. Therefore, this UTN-model-based prediction method is more suitable for PtMS than the traditional prediction methods.

Nonetheless, this prediction model still requires several known parameters (current number of the waiting vehicles at the stop line, traffic flow feeding in the network in the future, etc.) as input variables. However, obtaining the exact values of these parameters is usually very difficult. Therefore, the further steps of this paper are to find the method to acquire more precise values of these required parameters, as well as to test this model in real-world urban-road networks.

In addition, the proposed traffic-predicting UTN model can be also substituted with other traffic models, such as the model proposed by

Flotterod and Rohde [18]. Therefore, we will attempt to extend the model of Flotterod and Rohde for the traffic flow prediction of UTNs in the future and make a comparison with the results of this paper.

REFERENCES

[1] F.-Y. Wang, "Parallel control and management for intelligent transportation systems: Concepts, architectures, and applications," *IEEE Trans. Intell. Transp. Syst.*, vol. 11, no. 3, pp. 630–638, Sep. 2010.

[2] G. Xiong, S. Liu, X. Dong, F. Zhu, B. Hu, D. Fan, and Z. Zhang, "Parallel traffic management system helps 16th Asian games," *IEEE Intell. Syst.*, vol. 27, no. 3, pp. 74–78, May/Jun. 2012.

[3] I. Okutani and Y. J. Stephanedes, "Dynamic prediction of traffic volume through Kalman filtering theory," *Transp. Res. B*, vol. 18, no. 1, pp. 1–11, Feb. 1984.

[4] B. L. Smith, B. M. Williams, and R. K. Oswald, "Comparison of parametric and nonparametric models for traffic flow forecasting," *Transp. Res. C*, vol. 10, no. 4, pp. 303–321, Aug. 2002.

[5] M. M. Hamed, H. R. Al-Masaeid, and Z. M. Bani Said, "Short-term prediction of traffic volume in urban arterials," *J Transp. Eng.*, vol. 121, no. 3, pp. 249–254, May 1995.

[6] E. I. Vlahogianni, M. G. Karlaftis, and J. C. Golias, "Optimized and meta-optimized neural networks for short-term traffic flow prediction: A genetic approach," *Transp. Res. C*, vol. 13, no. 3, pp. 211–234, Jun. 2005.

[7] A. Stathopoulos, L. Dimitriou, and T. Tsekeris, "Fuzzy modeling approach for combined forecasting of urban traffic flow," *Comput.-Aided Civil Infrastruct. Eng.*, vol. 23, no. 7, pp. 521–535, Oct. 2008.

[8] S. Sun, C. Zhang, and G. Yu, "A Bayesian network approach to traffic flow forecasting," *IEEE Trans. Intell. Transp. Syst.*, vol. 7, no. 1, pp. 124–132, Mar. 2006.

[9] E. I. Vlahogianni, M. G. Karlaftis, and J. C. Golias, "Spatio-temporal short-term urban traffic volume forecasting using genetically optimized modular networks," *Comput.-Aided Civil Infrastruct. Eng.*, vol. 22, no. 5, pp. 317–325, Jul. 2007.

[10] W. Min and L. Wynter, "Real-time road traffic prediction with spatio-temporal correlations," *Transp. Res. C*, vol. 19, no. 4, pp. 606–616, Aug. 2011.

[11] S. Lin, Y. Xi, and Y. Yang, "Short-term traffic flow forecasting using macroscopic urban traffic network model," in *Proc. 11th Int. IEEE Conf. Intell. Transp. Syst.*, Beijing, China, 2008, pp. 134–138.

[12] S. Lin and Y. Xi, "An efficient model for urban traffic network control," in *Proc. 17th IFAC World Congr.*, Seoul, Korea, 2008, pp. 14 066–14 071.

[13] M. Van den Berg, A. Hegyi, B. De Schutter, and J. Hellendoorn, "Integrated traffic control for mixed urban and freeway networks: A model predictive control approach," *Europ. J. Transp. Infrastruct. Res.*, vol. 7, no. 3, pp. 223–250, Sep. 2007.

[14] *Traffic Software Integrated System Version 5.1 User's Guide*, Fed. Highway Admin., Washington, DC, USA, 2001.

[15] R. J. Hyndman and A. B. Koehler, "Another look at measures of forecast accuracy," *Int. J. Forecast.*, vol. 22, no. 4, pp. 679–688, Oct.–Dec. 2006.

[16] B. D. Greenshields, "A study of traffic capacity," in *Proc. Ann. Meeting Highway Res. Board*, 1935, vol. 14, pp. 448–477.

[17] M. J. Lighthill and G. B. Whitham, "On kinematic waves II: A theory of traffic flow on long crowded roads," *Proc. Roy. Soc. Lond. Ser. A*, vol. 229, no. 1178, pp. 317–345, May 1955.

[18] G. Flotterod and J. Rohde, "Operational macroscopic modeling of complex urban road intersections," *Transp. Res. B*, vol. 45, no. 6, pp. 903–922, Jul. 2011.

Studying the Effects of Driver Distraction and Traffic Density on the Probability of Crash and Near-Crash Events in Naturalistic Driving Environment

Renran Tian, Lingxi Li, *Member, IEEE*, Mingye Chen, Yaobin Chen, *Senior Member, IEEE*, and Gerald J. Witt

***Abstract*—Driver distraction detection and intervention are important for designing modern driver-assistance systems and for improving safety. The main research question of this paper is to investigate how the cumulative driver off-road glance duration can be controlled to reduce the probability of occurrences of crash and near-crash events. Based on the available data sets from the Virginia Tech Transportation Institute (VTTI) 100-car study, the conditional probability is calculated to study the chance of crash and near-crash events when the given cumulative off-road glance duration in 6 s has been reached. Different off-road eye-glance locations and traffic density levels are also evaluated. The results show that one linear relationship can be obtained between the cumulative off-road eye-glance duration in 6 s and the risk of occurrences of crash and near-crash events, which varies for different off-road eye-glance locations. In addition, the traffic density level is found to be one significant moderator to this linear relationship. Detailed comparisons are made for different traffic density levels, and one nonlinear equation is obtained to predict the probability of occurrences of crash and near-crash events by considering both cumulative off-road glance duration and traffic density levels.**

***Index Terms*—Cumulative driver off-road glance duration, driver distraction, human factors, naturalistic driving environment, traffic density.**

I. INTRODUCTION

DRIVER distraction is one of the most widely known prominent contributors to traffic accidents [1]. Based on the attention-competing model between road demand and concurrent secondary tasks [1]–[3], researchers tried to explain the underlying mechanism causing degraded driving performance and summarize empirical evidences of the effects of distraction on driving safety. According to one naturalistic driving study reported in [1], about 25% of police-reported cases [2] and 65%–80% of crash and near-crash cases have driver distraction and/or driver inattention involved as contributors. In [2]–[5], the relationship between external/internal driver distraction sources and driving safety/performance measures in different environments are investigated. It is clear that many kinds of distracted driving behaviors are associated with specified driving safety degradation.

Extensive research has been done to detect driver distraction and to design preventive systems to improve driving safety. According to the work in [5], the most commonly used inputs to detect driver distraction include driver biological measures [6], [7], driver physical measures [6]–[15], and driving performance measures [8]–[10], [15], [16]. It is noticeable that, for most of the comprehensive models, the detection of driver distraction is essentially based on the driver physical measures,

Manuscript received January 3, 2013; revised March 20, 2013; accepted April 20, 2013. Date of publication May 23, 2013; date of current version August 28, 2013. The Associate Editor for this paper was Dr. Q. Kong.

R. Tian, L. Li, M. Chen, and Y. Chen are with the Department of Electrical and Computer Engineering and also with the Transportation Active Safety Institute, Indiana University–Purdue University Indianapolis, Indianapolis, IN 46202 USA (e-mail: rtian@iupui.edu; ll7@iupui.edu; chen306@iupui.edu; ychen@iupui.edu).

G. J. Witt is with the Delphi Electronics and Safety, Kokomo, IN 46092 USA (e-mail: Gerald.J.Witt@delphi.com).

Color versions of one or more of the figures in this paper are available online at http://ieeexplore.ieee.org.

Digital Object Identifier 10.1109/TITS.2013.2261988

1524-9050 © 2013 IEEE